Effects of *d*-band shape on the surface reactivity of transition-metal alloys

Hongliang Xin,[1,2] Aleksandra Vojvodic,[1] Johannes Voss,[1] Jens K. Nørskov,[1,2] and Frank Abild-Pedersen[1,*]

[1]*SUNCAT Center for Interface Science and Catalysis, SLAC National Accelerator Laboratory, 2575 Sand Hill Road, Menlo Park, California 94025, United States*

[2]*Department of Chemical Engineering, Stanford University, Stanford, California 94305, United States*

(Received 13 January 2014; revised manuscript received 28 February 2014; published 13 March 2014)

The *d*-band shape of a metal site, governed by the local geometry and composition of materials, plays an important role in determining trends of the surface reactivity of transition-metal alloys. We discuss this phenomenon using the chemisorption of various adsorbates such as C, N, O, and their hydrogenated species on Pd bimetallic alloys as an example. For many alloys, the *d*-band center, even with consideration of the *d*-band width and *sp* electrons, can not describe variations in reactivity from one surface to another. We investigate the effect of the *d*-band shape, represented by higher moments of the *d* band, on the local electronic structure of adsorbates, e.g., energy and filling of adsorbate-metal antibonding states. The upper *d*-band edge ε_u, defined as the highest peak position of the Hilbert transform of the density of states projected onto *d* orbitals of an active metal site, is identified as an electronic descriptor for the surface reactivity of transition metals and their alloys, regardless of variations in the *d*-band shape. The utilization of the upper *d*-band edge with scaling relations enables a considerable reduction of the parameter space in search of improved alloy catalysts and further extends our understanding of the relationship between the electronic structure and chemical reactivity of metal surfaces.

DOI: 10.1103/PhysRevB.89.115114 PACS number(s): 73.20.At, 82.65.+r, 68.43.−h

I. INTRODUCTION

The making and breaking of chemical bonds of molecules or their fragments at solid materials is the basis for many technological applications, such as self-assembled molecular coatings, corrosion protection, chemical sensing, and heterogeneous catalysis [1–3]. Realization of those functionalities with optimized performance and minimal cost by materials design relies on a fundamental understanding of the electronic structure of an ensemble of surface atoms and its relationship with energetics of adsorbate-surface interactions [4–7]. For that matter, identification of simple reactivity descriptors from complex electronic properties of materials becomes tremendously important. Such a simplification often leads to key concepts that can provide guidance in tailoring the geometry and composition of surface atoms for desired properties. The *d*-band center ε_d, i.e., the average energy of electronic *d* states projected onto a surface metal atom, is such a descriptor within the theoretical framework of the *d*-band model of surface chemisorption [5,8,9]. During the last two decades, the *d*-band model has been widely used to understand variations in chemisorption energies of various adsorbates on transition-metal surfaces and their alloys [10–12]. In general, a metal site with a higher (lower) *d*-band center exhibits stronger (weaker) affinity to adsorbates due to decreased (increased) filling of adsorbate-metal antibonding states. This simple design principle has proven to be extremely useful in search of optimal catalytic materials in many chemical and electrochemical reactions [13–15].

Outliers from the *d*-band model exist when the *d*-band center of an active site is used as a reactivity descriptor for metal surfaces [9,16–18], i.e., increasing (decreasing) the *d*-band center of a metal site is not always associated with stronger (weaker) chemical bonding. To extend the *d*-band model for understanding some of those discrepancies, a generalized electronic descriptor ε_d^W defined as $\varepsilon_d + W_d/2$ where W_d is the width of the *d* band of a surface metal atom, has been identified as an improved reactivity descriptor for pristine transition metals [18]. This descriptor, representing the upper edge of the *d* band, takes into account the effects of not only the average energy of *d* states but also their spread in energy on the position of adsorbate-metal antibonding states. Herein, we show that the *d*-band shape of a metal site plays an important role in determining the local surface reactivity of transition-metal alloys. We have studied a series of Pd alloys where the *d*-band center, even with consideration of the *d*-band width [18] and *sp* electrons [16], is not sufficient to understand trends of their surface reactivity, which indicates the need for a better descriptor. Effects of the *d*-band shape on the local electronic structure of adsorbates were explored based on the Newns-Anderson model. We found that the upper *d*-band edge ε_u, defined as the highest peak position of the Hilbert transform of the density of states (DOS) projected onto *d* orbitals of an active metal site, is a good reactivity descriptor for late transition metals and their alloys, regardless of variations in the *d*-band shape. By combining the ε_u with scaling relations [19,20] between adsorption energies of simple adsorbates and that of their hydrogenated species, it will be possible for predicting surface reaction energies on locally perturbed metal sites, for example, through alloying. Acetylene (C_2H_2) hydrogenation reactions on Pd alloys were used to exemplify the approach. A remarkable agreement between the model prediction and self-consistent density functional theory (DFT) calculations is observed. This approach could enable a considerate reduction of the parameter space in search of improved alloy catalysts.

II. COMPUTATIONAL DETAILS

All adsorption energies shown here are calculated using QUANTUM ESPRESSO [21] with ultrasoft pseudopotentials and

*abild@slac.stanford.edu

the BEEF-vdW [22] density functional that explicitly includes van der Waals dispersion interactions. A 2 × 2 × 4 slab model is used with 1/4 ML adsorbate coverage at the atop site for simple adsorbates (C, N, and O) and the most favorable sites for CH_3 (atop) and hydrogenated C_2 species. The atop site was used for the adsorption of atomic species only for the purpose of probing the local surface reactivity of alloy materials. The adsorbate and the top two layers of surface atoms are fully relaxed until the forces are smaller than 0.05 eV/Å. The Brillouin zones of all surfaces were sampled with 6 × 6 × 1 Monkhorst-Pack k points [23]. The kinetic energy cutoff for plane-wave basis sets was 500 eV. The calculation parameters were chosen to ensure that the adsorption energies are converged within 0.1 eV. Gaussian broadening 0.2 eV was used for calculating DOS spectra.

III. RESULTS AND DISCUSSION

Figure 1 shows DFT-calculated binding energies for C, N, and O on the (111) surface of Pd and Pd/X alloys (X represents late transition metals Cu, Ag, Au, Ni, Pd, Pt, Co, Rh, and Ir) as a function of the d-band center (see Table I for details). Interestingly, the binding energies of C, N, and O on Pd and Pd/X alloys show a V-shaped relationship with ε_d. For alloy systems located in the left region where some of the late transition metals (Cu, Ni, Pd, Pt, Co, Rh, and Ir) are involved in the Pd lattice, the adsorbate-Pd bond becomes stronger as ε_d of the active site moves up in energy. This is in line with the general prediction of the d-band model. However, outliers emerge in the right region where Pd is alloyed with Ag or Au, i.e., the chemical bond becomes weaker as ε_d moves up in energy. The lack of a generalized reactivity descriptor for transition-metal alloys within the field of surface chemistry is worrisome, and also poses a grand challenge for the rational catalyst design based on electronic descriptors [14,15].

To understand the local electronic structure of alloy materials and possibly identify a better reactivity descriptor, we show

TABLE I. Tabulated data for the electronic structure of the d band projected onto a surface Pd atom and adsorption energies (units in eV).

Surface	ε_d	ε_u	ΔE_C	ΔE_N	ΔE_O
Pd	−1.61	0.11	4.60	3.77	2.65
Pd_3Cu	−1.67	−0.34	5.00	3.98	2.83
Pd_3Ag	−1.48	−0.35	4.90	3.87	2.74
Pd_3Au	−1.49	−0.07	4.87	3.92	2.85
Pd_3Ni	−1.80	0.11	4.93	3.95	2.77
Pd_3Pt	−1.67	0.08	4.75	3.90	2.81
Pd_3Co	−1.93	−0.70	5.13	4.05	2.81
Pd_3Rh	−1.79	0.04	4.79	3.93	2.72
Pd_3Ir	−1.91	−0.12	4.97	4.05	2.90
Pd_2Cu_2	−1.74	−0.33	5.20	4.13	2.91
Pd_2Ag_2	−1.39	−0.37	5.07	4.00	2.77
Pd_2Au_2	−1.42	−0.26	5.11	4.10	3.00
Pd_2Ni_2	−2.03	−0.40	5.11	4.02	2.81
Pd_2Pt_2	−1.75	0.10	4.89	4.02	2.95
Pd_2Co_2	−2.26	−0.85	5.30	4.13	2.82
Pd_2Rh_2	−1.93	0.10	4.85	3.94	2.74
Pd_2Ir_2	−2.13	−0.17	5.11	4.16	3.00
$PdCu_3$	−1.99	−0.77	5.40	4.30	2.91
$PdAg_3$	−1.50	−1.03	5.19	4.13	2.71
$PdAu_3$	−1.39	−0.60	5.29	4.24	3.04
$PdNi_3$	−2.27	−0.41	5.23	4.09	2.88
$PdPt_3$	−1.80	0.12	4.97	4.08	3.06
$PdCo_3$	−2.48	−0.93	5.36	4.18	2.81
$PdIr_3$	−2.43	−0.91	5.18	4.19	3.04

in Fig. 2(a) the DOS projected onto the Pd 4d orbitals of clean Pd/Ag alloys (as an example) and C 2p orbitals of C on Pd/Ag alloys with varying Pd/Ag atomic ratios. Although the d-band center ε_d of the surface Pd atoms shown in Fig. 2 (marked as vertical lines) shifts up slightly in energy when forming alloys, the C_{2p}-Pd_{4d} antibonding states move down toward the Fermi level and get more occupied, i.e., the C-Pd bond weakens upon

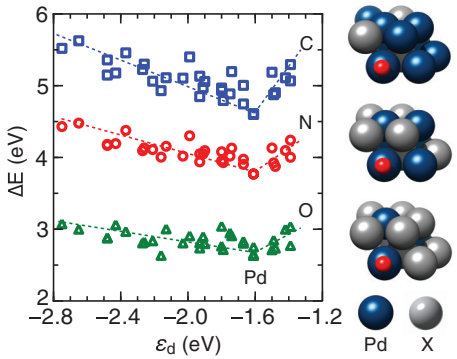

FIG. 1. (Color online) (a) Adsorption energies of C, N, and O on the (111) surface (atop site) of Pd and Pd/X alloys as a function of the ε_d of surface Pd atoms. Dashed lines are used to guide the eye and separate two regions of adsorption energies with different correlations to the ε_d. Adsorption energies are referenced to their gas phase hydrogenated species CH_4, NH_3, H_2O, and H_2. 3:1, 2:2, and 1:3 atomic ratios of Pd/X (X: late transition metals) are used in alloys, and the corresponding geometries (Pd_3X, Pd_2X_2, and PdX_3) are shown with an adsorbate at the atop site of Pd.

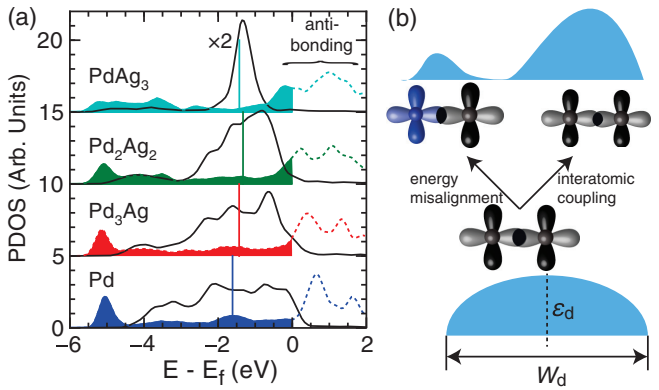

FIG. 2. (Color online) (a) Projected DOS onto Pd 4d orbitals (solid lines) of clean Pd and Pd/Ag alloys and C 2p orbital (dashed lines) of C on Pd and Pd/Ag alloys. The vertical solid lines are used to denote the d-band center of a surface Pd atom in the (111) surface of Pd and Pd alloys. (b) Schematic illustration of the underlying mechanisms (e.g., energy misalignment and interatomic coupling) for variations in the d-band shape upon formation of alloys.

alloying Pd with Ag. Furthermore, the variations in binding energies become more pronounced as the concentration of the guest element in the alloy increases. The same phenomenon was also observed for Pd/Au alloys. We note that for the adsorbate/substrate systems studied here, a weakening of a chemical bond is typically associated with a longer adsorbate-metal bond length, i.e., smaller interatomic coupling matrix element V_{ad} [24]. This suggests that the trend of surface reactivity is not governed by the repulsive interaction ($\propto V_{ad}^2$) resulting from orbital orthogonalization between renormalized adsorbate states and metal d states [16]. Since the sp band of transition metals and their alloys is broad and similar, the chemisorption energy due to its interaction with a specific adsorbate valence state is approximately constant [3]. All this indicates that the orbital hybridization of the renormalized adsorbate states with the metal d states due to variations in the fine structure of the d band, e.g., the shape, is what gives rise to the outliers and the V-shaped relationships for chemisorption observed in Fig. 1.

To further explore the electronic origin of the V-shaped relationships discussed above, it is critical to investigate the band characteristics of the d-DOS projected onto a surface Pd atom in pure Pd and Pd alloys. One can see in Fig. 2(a) that the distribution of d states for pure Pd is largely symmetric and relatively flat (no sharp peaks). When forming alloys, the d-DOS of a surface Pd atom is dramatically modified. For the case of Pd/Ag alloys, a narrow band arises at high energies (~ -1.8 eV relative to the Fermi level) and a tail emerges at low energies (~ -4.0 eV). The width of the d-DOS, quantified by its second central moment, of a surface Pd atom barely changes (see Appendix for detailed discussion about moments of electronic states). However, higher moments of the d band, characterizing the shape of the distribution of d states [25], such as skewness and kurtosis, change dramatically. The underlying mechanisms of those changes are illustrated in Fig. 2(b). For pristine transition metals, the d states projected onto a surface atom can be approximated as a semielliptical distribution centered at ε_d with width W_d. However, for transition-metal alloys, such as Pd/Ag and Pd/Au, there is the formation of electronic states away from the ε_d mainly due to the energy misalignment of interacting d orbitals. Concurrently, sharper (broader) peaks might emerge because of variations in the spatial extent of interacting d orbitals. In the perturbed chemical environment by guest metal atoms, the d orbitals of neighboring atoms can become more contracted (extended) and that leads to changes in the interatomic coupling matrix elements V_{dd}, and hence the d-band moments [24]. These substantial changes in the d-band characteristics make it crucial to take into account the effects of the d-band shape for understanding trends of the local surface reactivity of transition-metal alloys.

To pinpoint the underlying factors governing the surface reactivity of transition-metal alloys, we employed the Newns-Anderson model to describe the hybridization between renormalized adsorbate states with a distribution of electronic d states of the substrate [26–28]. We show in Fig. 3(a) the Hilbert transform of the d-DOS of a surface Pd atom in Pd and Pd/Ag alloys. Within the Newns-Anderson model, the intersects of the adsorbate function ($y = \varepsilon - \varepsilon_a$) with the substrate function determine the positions of adsorbate-metal

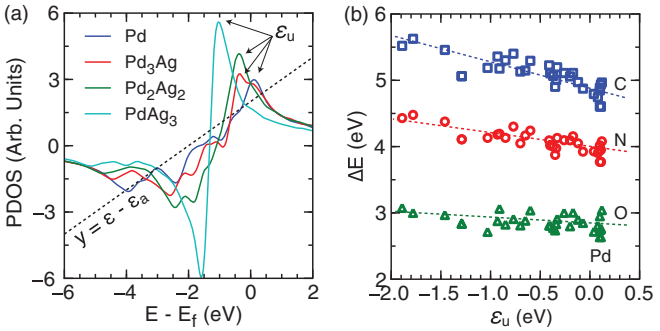

FIG. 3. (Color online) (a) The Hilbert transform of the local d-DOS of surface Pd atoms in Pd and Pd/Ag alloys. Dashed line represents the adsorbate function $y = \varepsilon - \varepsilon_a$, where ε_a is the center of the renormalized adsorbate states formed after the interaction of an adsorbate valence level in vacuum with the sp band of the substrate. The intersects of the adsorbate function with the upper part of the Hilbert transform of the d-DOS projected onto a surface Pd atom represent the adsorbate-metal antibonding states. The upper d-band edge ε_u, defined as the highest peak position of the Hilbert transform of the local d-DOS, is marked with arrows. (b) Adsorption energies of C, N, and O on Pd and Pd alloys with late transition metals at 3:1, 2:2, and 1:3 atomic ratios as a function of the ε_u.

bonding and antibonding states. ε_a is the center energy of the renormalized adsorbate states (e.g., ~ -2.0 eV for C), calculated from the projected p-DOS of adsorbates on a Na(110) surface. The substrate function is defined as the Hilbert transform of the d-DOS of a surface Pd atom, assuming a constant interatomic coupling matrix element V_{ad}^2 for alloys. The lowering of the adsorbate-metal antibonding state leads to higher filling and hence weaker chemical bonding. It should be noted that the position of the adsorbate-metal antibonding states is adsorbate dependent since the adsorbate function depends on the position of renormalized adsorbate states ε_a and the substrate function is proportional to the adsorbate-metal interatomic coupling matrix elements [taken as 1 in Fig. 3(a)]. To identify a simple reactivity descriptor that is only dependent on the local electronic structure of the substrate and determines the relative position of the metal-adsorbate antibonding state, we use the highest peak position of the Hilbert transform of the d-DOS to define the upper d-band edge ε_u,

$$\varepsilon_u = \underset{\varepsilon}{\operatorname{argmax}} \frac{1}{\pi} P \int_{-\infty}^{\infty} \frac{\rho(\varepsilon')}{\varepsilon - \varepsilon'} d\varepsilon', \tag{1}$$

where P represents the principal value of the integral. The Hilbert transform was determined using *scipy.signal.hilbert* from the SCIPY package (www.scipy.org). The main observation in Fig. 3(a) is that the positions of the adsorbate-metal antibonding states shift synchronously with the ε_u. To test the validity of ε_u as a reactivity descriptor, Fig. 3(b) shows the binding energies of C, N, and O on Pd and Pd alloys as a function of the ε_u. Considering the simplicity of the descriptor, the linear correlations shown in Fig. 3(b) are striking. In particular, the adsorption energies of C, N, and O on alloy systems (Pd/Ag and Pd/Au) correlates very well with the upper d-band edge (see Table I for details).

We show in Fig. 4 that the ε_u also correlates linearly with adsorbate (e.g., CH_3) binding energies on pristine transition

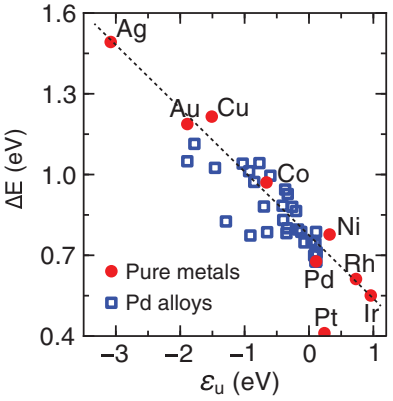

FIG. 4. (Color online) The adsorption energies of CH_3 on pure transition metals and Pd alloys as a function of the upper d-band edge ε_u of surface active atoms.

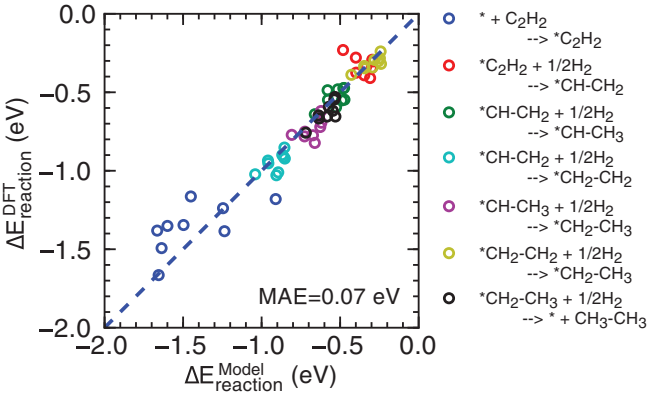

FIG. 5. (Color online) DFT-calculated reaction energies of a series of hydrogenation reactions of acetylene (C_2H_2) plotted against the model prediction on various Pd_3X alloys using the established correlation between the upper d-band edge ε_u and C binding energies, together with scaling relations between the binding energy of C and hydrogenated C_2 species.

metals. This is because the d-DOS of transition metals can be well represented by a semielliptical shape function and the analytic expression of $\varepsilon_d + W_d/2$, to a first approximation, defines the upper d-band edge. These linear relationships suggest that the ε_u can be used as a reactivity descriptor for late transition metals and their alloys, regardless of variations in d-band shape. However, we can not completely rule out the effect of the adsorbate-metal coupling matrix elements V_{ad} that might play an important role for some adsorbates, e.g., F, Cl, and OH, particularly on substrates of metals with extended d orbitals [16,24] and/or large difference in electronegativity [29].

Given on one hand the linear relationship between the upper d-band edge ε_u and binding energies of simple adsorbates C, N, and O, and on the other hand scaling relations between the binding energies of those adsorbates and their hydrogenated species [19], it is possible to predict energetics of hydrogenation and dehydrogenation reactions on alloys using only the ε_u of the surface Pd site in alloys. The hydrogenation of unsaturated molecules represents a key reaction in heterogeneous catalysis with very broad applications [30]. We demonstrate the usage of the ε_u for predicting energetics of C_2H_2 hydrogenation reactions on Pd alloys as shown in Fig. 5. We used the simple linear correlation of C binding energies with the ε_u,

$$\delta\Delta E_C = \gamma_C \delta\varepsilon_u, \tag{2}$$

where γ_C is -0.93 for C on Pd alloys obtained from Fig. 3(b) with linear regression ($R^2 = 0.9$). The change of binding energies of C_2 species was then estimated based on scaling relations

$$\delta\Delta E_{C_2H_y} = (6-y)/4\,\delta\Delta E_C, \tag{3}$$

where $(6-y)$ and 4 represent valency of C_2H_y and C species, respectively [20,31]. The reaction energies predicted with Eqs. (2) and (3), i.e., using the ε_u as a descriptor, are in excellent agreement with self-consistent DFT calculations. The mean absolute error (MAE) is 0.07 eV to be compared with 0.15 eV using ε_d as a descriptor. With this approach, it is also possible to establish the full potential energy surfaces for metal alloys by combining with the Brønsted- Evans-Polanyi (BEP) relationship [32] between reaction energies and activation barriers.

IV. CONCLUSIONS

In conclusion, electronic factors governing the trend of surface reactivity of transition-metal alloys have been revisited to include the effects of the d-band shape. The upper d-band edge ε_u, defined as the highest peak position of the Hilbert transform of the d-DOS projected onto an active metal site, is identified as an electronic descriptor for the surface reactivity of pure transition metals and their alloys. The finding furthers our understanding of chemical bonding on metal surfaces where the local electronic structure is perturbed, for example, through alloying. With scaling relations, it is possible to screen through a large phase space of bimetallic and multimetallic materials based on the ε_u, greatly reducing the parameter space in search of improved catalysts.

ACKNOWLEDGMENT

The authors gratefully acknowledge the Financial support from the US Department of Energy, Office of Basic Energy Sciences to the SUNCAT Center for Interface Science and Catalysis.

APPENDIX

In general, for a given distribution of projected d-DOS, $\rho(\varepsilon)$, important information about the characteristics of local electronic structure [25], e.g., the number of d states (n_d), the d-band center (ε_d), the d-band width (W_d), and the d-band shape, can be described by its power moments μ_n defined as

$$\mu_n = \int (\varepsilon - \varepsilon_d)^n \rho(\varepsilon) d\varepsilon, \quad n = 0,1,2,3,4,\ldots, \tag{A1}$$

where the d-band center ε_d is typically used as the reference for moments of d-DOS. In essence, the moments of projected d-DOS are determined by the local geometry and the composition of materials [25], and the nth moment is directly

related to the product of matrix elements of the operator $H - \varepsilon_d$, for n-step electron hopping paths ($i_0 \rightarrow i_1$, $i_1 \rightarrow i_2$, $\ldots$, $i_{n-1} \rightarrow i_0$),

$$\mu_n = \sum_{i_1, i_2, \ldots i_{n-1}} \langle i_0 | H - \varepsilon_d | i_1 \rangle \langle i_1 | H - \varepsilon_d | i_2 \rangle \ldots \langle i_{n-1} | H - \varepsilon_d | i_0 \rangle , \quad \text{(A2)}$$

where the summation is over all length-n electron hopping paths starting and ending in a targeted lattice site i_0. In Eq. (A2), H is the Hamiltonian of the system defined as $\sum_k |\Phi_k\rangle \varepsilon_k \langle \Phi_k|$ including all eigenstate $\langle k|$ with eigenfunction Φ_k. μ_0 is simply an integration of the local density of states, giving no information for a normalized distribution. The first moment μ_1, characterizing the average energy of the distribution, is zero in this definition. The square root of the second moment $\mu_2^{1/2}$ characterizes the width of the distribution relative to the center of gravity ε_d. The asymmetry and heavy tails of the distribution can be represented by standard third (skewness) and fourth moments (kurtosis), defined as $\mu_3/\mu_2^{3/2}$ and μ_4/μ_2^2, respectively.

[1] T. N. Rhodin and G. Ertl, *The Nature of the Surface Chemical Bond* (North-Holland, Amsterdam, 1979).

[2] R. A. van Santen and M. Neurock, *Molecular Heterogeneous Catalysis: A Conceptual and Computational Approach* (Wiley-VCH, Weinheim, 2006).

[3] A. Nilsson, L. Pettersson, and J. K. Nørskov, *Chemical Bonding at Surfaces and Interfaces* (Elsevier, Amsterdam, 2008).

[4] B. I. Lundqvist, O. Gunnarsson, H. Hjelmberg, and J. K. Nørskov, Surf. Sci. **89**, 196 (1979).

[5] B. Hammer and J. K. Nørskov, Adv. Catal. **45**, 71 (2000).

[6] J. Greeley, J. K. Nørskov, and M. Mavrikakis, Annu. Rev. Phys. Chem. **53**, 319 (2002).

[7] H. Xin, A. Holewinski, N. Schweitzer, E. Nikolla, and S. Linic, Top. Catal. **55**, 376 (2012).

[8] B. Hammer and J. K. Nørskov, Surf. Sci. **343**, 211 (1995).

[9] B. Hammer and J. K. Nørskov, Nature (London) **376**, 238 (1995).

[10] M. Mavrikakis, B. Hammer, and J. K. Nørskov, Phys. Rev. Lett. **81**, 2819 (1998).

[11] J. R. Kitchin, J. K. Nørskov, M. A. Barteau, and J. G. Chen, Phys. Rev. Lett. **93**, 156801 (2004).

[12] J. R. Kitchin, J. K. Nørskov, M. A. Barteau, and J. G. Chen, J. Chem. Phys. **120**, 10240 (2004).

[13] B. Hammer, Top. Catal. **37**, 3 (2006).

[14] J. K. Nørskov, T. Bligaard, J. Rossmeisl, and C. H. Christensen, Nat. Chem. **1**, 37 (2009).

[15] J. K. Nørskov, F. Abild-Pedersen, F. Studt, and T. Bligaard, Proc. Natl. Acad. Sci. USA **108**, 937 (2011).

[16] H. Xin and S. Linic, J. Chem. Phys. **132**, 221101 (2010).

[17] F. Calle-Vallejo, J. I. Martínez, J. M. García-Lastra, J. Rossmeisl, and M. T. M. Koper, Phys. Rev. Lett. **108**, 116103 (2012).

[18] A. Vojvodic, J. K. Nørskov, and F. Abild-Pedersen, Top. Catal. **57**, 25 (2014).

[19] F. Abild-Pedersen, J. Greeley, F. Studt, J. Rossmeisl, T. R. Munter, P. G. Moses, E. Skulason, T. Bligaard, and J. K. Nørskov, Phys. Rev. Lett. **99**, 016105 (2007).

[20] G. Jones, F. Studt, F. Abild-Pedersen, J. K. Nørskov, and T. Bligaard, Chem. Eng. Sci. **66**, 6318 (2011).

[21] P. Giannozzi, S. Baroni, N. Bonini, M. Calandra, R. Car, C. Cavazzoni, D. Ceresoli, G. L. Chiarotti, M. Cococcioni, I. Dabo *et al.*, J. Phys.: Condens. Matter **21**, 395502 (2009).

[22] J. Wellendorff, K. T. Lundgaard, A. Møgelhøj, V. Petzold, D. D. Landis, J. K. Nørskov, T. Bligaard, and K. W. Jacobsen, Phys. Rev. B **85**, 235149 (2012).

[23] H. J. Monkhorst and J. D. Pack, Phys. Rev. B **13**, 5188 (1976).

[24] W. A. Harrison, *Electronic Structure and the Properties of Solids: The Physics of the Chemical Bond* (Dover, New York, 1989).

[25] A. P. Sutton, *Electronic Structure of Materials* (Oxford University Press, Oxford, UK, 1993).

[26] P. W. Anderson, Phys. Rev. **124**, 41 (1961).

[27] D. M. Newns, Phys. Rev. **178**, 1123 (1969).

[28] J. P. Muscat and D. M. Newns, Prog. Surf. Sci. **9**, 1 (1978).

[29] H. Xin, A. Holewinski, and S. Linic, ACS Catal. **2**, 12 (2012).

[30] F. Delbecq, D. Loffreda, and P. Sautet, J. Phys. Chem. Lett. **1**, 323 (2010).

[31] B. Liu and J. Greeley, J. Phys. Chem. C **115**, 19702 (2011).

[32] T. Bligaard, J. K. Nørskov, S. Dahl, J. Matthiesen, C. H. Christensen, and J. Sehested, J. Catal. **224**, 206 (2004).